

INFLUENCE OF DAMAGE ONSET AND PROPAGATION ON THE TENSILE STRUCTURAL BEHAVIOUR OF PROTRUDING COMPOSITE JOINTS

A. Riccio* and F. Scaramuzzino⁺

*C.I.R.A. (Italian Aerospace Research Centre),
Via Maiorise, 81043 Capua, Italy

⁺Department of Aerospace and Mechanical Engineering,
II University of Naples,
Via Roma 29, 81031 Aversa, Italy

Keywords: composites, joints, contacts, progressive damage, failure criteria, FEM, degradation rules.

Abstract. *In the present paper, a detailed numerical investigation of the structural behaviour of single-lap protruding composite joints under tensile loading has been carried out using a three-dimensional progressive damage FEM model. The adopted FEM model is based on a combination of Hashin's failure Criteria, ply-discount material's degradation rules and penalty method (for contact-friction phenomena).*

Some joints' configurations with different hole's diameter and different interfaces (composite/composite and composite/aluminium) have been analysed. The numerical results in terms of strain curves, load-displacement curves and damage propagation have been compared with experimental data in order to point out the effectiveness and the weak points of the proposed progressive damage approach. Comparisons between the numerical damage and no-damage approach for each configuration have been carried out in order to analyse the influence of progressive damage approach on the numerical simulation of the overall structural behaviour. Also the influence of penalty contact stiffness on the damage onset and damage propagation inside the joints has been investigated. Finally, particular emphasis has been given to the damage onset and damage propagation inside the joints critically discussing the differences among the analysed geometrical configurations.

1 INTRODUCTION

Bolted joints are commonly used to assemble composite laminates in aircraft structures. The strength, the stiffness and the light-weight properties of composites make their use very attractive, but the brittle failure, characterising their structural behaviour, is a real obstacle to the development of a fully composite oriented design philosophy. Hence a deep understanding of their strength and failure modes is very important in order to provide reliable design of bolted joints in composite structures.

The Composite joints structural behaviour has been predicted by a considerable number of authors by using different techniques. Several investigators have developed analytical procedures for calculating the strength of bolted joints in composite materials^[1-6]. All this investigations provide conservative results in terms of failure strength and with the exception of Agarwal's method^[2], none of the previous models can predict the mode of failure.

In [7] a method for the prediction of failure strengths and failure modes of fibre reinforced composite laminates containing one or two pin-loaded holes is proposed. This method is based on the combined use of a two-dimensional (2-D) finite element model and the Yamada-Sun failure criterion^[8].

More sophisticated two-dimensional finite element models are proposed in [9-10]. These models take into account the progression of damage in the joined composite plates by using the Hashin's failure criteria^[11], penalty approach for contact analysis^[12] and the ply discount method^[13] for properties degradation. However the 2-D approaches were found to give inconsistent results when dealing with the bearing failure mode due to its inherent 3-D nature. An attempt to bypass this limitation is presented in [14] where a modified 2-D finite element model based on the overlaid plane stress elements is introduced in order to analyse the bearing behaviour of a pinned composite joint.

A fully three-dimensional (3-D) finite element model for composite joints is proposed by other investigators^[15-18]. The stress distribution around a single composite bolt is investigated in [15], while in [16] the

3-D FEM model is used to predict the delamination onset in composite joints under bearing load. A very detailed FEM analysis of single-lap, single bolts composite joints is carried out in [17] where the stress distributions around the composite fasteners are calculated in order to predict the strength by using appropriate failure criteria. Finally in [18] an effective 3-D FEM approach based on a progressive damage model is adopted to investigate the damage accumulation in composite joints.

The present work is part of an extensive research started with the development of a two-dimensional progressive damage FEM approach for composite joints^[19]. This 2D approach was found to be ineffective when three-dimensional failure modes (like the bearing failure mode) were involved in computations. Hence the 2-D approach was revised and adapted to the three-dimensional formulation in [20-21]. The derived 3-D procedure is based on the geometrically non-linear finite element formulation for stress calculation. To impose friction contact conditions the penalty method and the Coulomb friction law have been adopted. The FEM model has finally been integrated with Hashin's failure criteria to split fibre and matrix failure modes and with the ply discount method to simulate the stiffness degradation in each ply.

In the present paper, the three-dimensional approach developed in [20-21], improved especially for what concerns the properties degradation rules, has been used to analyse the structural behaviour of single lap protruding composite joints under tensile loading.

In the next sections the theoretical basis of the implemented progressive damage procedure is briefly introduced and the results of numerical analyses on some joints' configurations with different hole's diameter and different interfaces (composite/composite and composite/aluminium) are shown.

First of all, the numerical results in terms of strain curves and load-displacement curves are compared with experimental data^[22] in order to verify the effectiveness and the weak points of the presented progressive damage approach. Then comparisons between the numerical damage and no-damage approaches for each configuration are introduced to point out the influence of progressive damage approach on the numerical simulation of the overall structural behaviour. Furthermore the importance of contact phenomena and the influence of penalty contact stiffness on the damage onset and damage propagation inside the joints is analysed in detail. Finally, the numerical damage onset and propagation is compared with ultrasonic NDE results and critically discussed for the analysed configurations.

2 THEORY

In this section, the theoretical background of the proposed progressive damage approach is introduced. The stress evaluation, the contact-friction analysis, the failure criteria application and the material properties degradation rules are components of the suggested formulation that need to be considered simultaneously for the simulation of the real structural behaviour of composite joints with damage on-set and propagation. In the following these components are briefly described.

2.1 Stress evaluation

For stress evaluation, large displacements and large rotations (Geometrical non-linearity) have been taken into account by means of the Green Lagrange strain tensor that, for the Updated Lagrangian Formulation, can be written:

$${}_t \mathbf{e}_{ij} = {}_t e_{ij} + {}_t \mathbf{h}_{ij} \quad (1)$$

with

$${}_t e_{ij} = \frac{1}{2} ({}_t u_{i,j} + {}_t u_{j,i}) \quad (2)$$

$${}_t \mathbf{h}_{ij} = \frac{1}{2} ({}_t u_{k,i} \cdot {}_t u_{k,j}) \quad (3)$$

where ${}_t e_{ij}$ and ${}_t \mathbf{h}_{ij}$ are respectively the linear and non linear part of strain tensor at time t and ${}_t u_{i,j} = \frac{\partial u_i}{\partial x_j}$.

2.2 Contact-friction analysis

Since the contact forces can strongly influence the stress distribution in the joints under investigation, the contact analysis can be considered of main importance in our computations.

In contact analysis, contacting forces are additional unknowns. The Penalty Method^[12] has been chosen for implementation in our model. The use of this method in conjunction with the Coulomb frictional law allows us to deal with contact-friction phenomena.

Using the Penalty formulation, if contact occurs a little overlapping ($GAP < 0$) between the two contact surfaces is allowed and the contact force F_C can be evaluated as a linear function of the GAP, according with

the following expression:

$$|F_c| = \mathbf{a} \cdot |GAP| \quad (4)$$

where \mathbf{a} is the penalty constant.

The major advantage of this technique is the reduced CPU time because no nested iteration is needed to calculate the contact forces. The major weak-point is related to the choice of \mathbf{a} : too low values of \mathbf{a} allow big over-lapping while too high values of \mathbf{a} can cause convergence problems in the solution of the non linear equilibrium equations. Hence a high degree of experience in the choice of penalty constants is needed to perform effective analyses with the Penalty Method.

To take into account the frictional contact forces, the Coulomb friction law is used:

$$|F_s| \leq \mu |F_N|. \quad (5)$$

It correlates friction contact force (F_s) to normal contact force (F_N) by means of frictional coefficient (μ). In relation (5) it is possible to distinguish the conditions of sticking contact ($|F_s| < \mu |F_N|$) and sliding contact ($|F_s| = \mu |F_N|$). Considering a contact pair (two points in contact representing two contacting surfaces), the adopted frictional approach is summarised in the Figure 1.

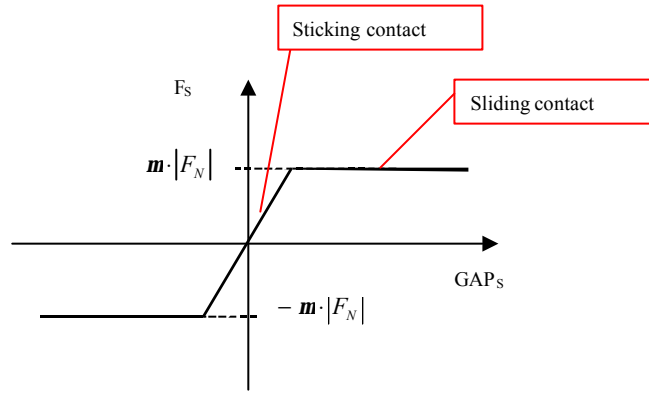


Figure 1. Frictional contact force as a function of the tangential distance between contacting points (GAP_s).

During the sticking contact, the frictional contact force is assumed to be a linear function of the tangential gap (GAP_s) between the points in contact. Using this assumption, due to a reasonable microscopic interpretation of the friction phenomenon, the static friction can be modelled as a linear spring^[12]. The sliding contact is modelled by simply introducing the constant tangential contribution $\mu |F_N|$ in the contact force.

2.3 Failure criteria application

From the stress distribution, by means of suitable failure criteria, it is possible to predict the location and the type of damage. In the present model the Hashin's failure criteria are adopted in order to predict separately the fibre breakage and the matrix cracking of each layer. In the Hashin's formulation distinct polynomials are associated to the different failure modes. In our three-dimensional problem, we have considered the following failure modes (\mathbf{s}_{ij} are the stress components in the ij direction and $S_{ij}, Y_t, X_t, Y_c, X_c$ are the material strengths):

- Matrix tensile failure ($\mathbf{s}_{yy} > 0$);

$$\left(\frac{\mathbf{s}_{yy}}{Y_t} \right)^2 + \left(\frac{\mathbf{s}_{xy}}{S_{xy}} \right)^2 + \left(\frac{\mathbf{s}_{yz}}{S_{yz}} \right)^2 \geq 1 \quad (6)$$

- Matrix compression failure ($\mathbf{s}_{yy} < 0$);

$$\left(\frac{\mathbf{s}_{xx}}{Y_t} \right)^2 + \left(\frac{\mathbf{s}_{xy}}{S_{xy}} \right)^2 + \left(\frac{\mathbf{s}_{xz}}{S_{yz}} \right)^2 \geq 1 \quad (7)$$

- Fibre tensile failure ($\mathbf{s}_{xx} > 0$);

$$\left(\frac{\mathbf{s}_{xx}}{X_t}\right)^2 + \left(\frac{\mathbf{s}_{xy}}{S_{xy}}\right)^2 + \left(\frac{\mathbf{s}_{xz}}{S_{xz}}\right)^2 \geq 1 \quad (8)$$

- Fibre compression failure ($\mathbf{s}_{xx} < 0$);

$$\left(\frac{\mathbf{s}_{xx}}{X_c}\right) \geq 1 \quad (9)$$

- Fibre-matrix shear-out failure ($\mathbf{s}_{xx} < 0$);

$$\left(\frac{\mathbf{s}_{xx}}{X_c}\right)^2 + \left(\frac{\mathbf{s}_{xy}}{S_{xy}}\right)^2 + \left(\frac{\mathbf{s}_{xz}}{S_{xz}}\right)^2 \geq 1 \quad (10)$$

- Fibre-Kinking failure ($\mathbf{s}_{xx} < 0$);

$$\left(\frac{\mathbf{s}_{xx}}{X_c}\right)^2 + \left(\frac{\mathbf{s}_{xz}}{S_{xz}}\right)^2 \geq 1 \quad (11)$$

2.4 Material properties degradation rules

The material properties degradation rules are applied to take into account the post damage material behaviour of each layer. This is necessary in order to perform a progressive failure analysis until global failure. For each of the above mentioned failure modes, according to the ply discount approach^[13], an appropriate property degradation rule was introduced reflecting the physics of the damage mechanisms.

- Matrix tensile and compression failure;

$$\begin{aligned} \bar{E}_y &= k \cdot E_y \\ \bar{E}_z &= k \cdot E_z \\ \bar{G}_{yz} &= k \cdot G_{yz} \end{aligned} \quad (12)$$

- Fibre tensile and compression failure;

$$\begin{aligned} \bar{E}_x &= k \cdot E_x \\ \bar{G}_{xy} &= G_{yz} \\ \bar{G}_{xz} &= G_{yz} \end{aligned} \quad (13)$$

- Fibre-matrix shear-out failure;

$$\begin{aligned} \bar{G}_{xy} &= G_{yz} \\ \bar{G}_{xz} &= G_{yz} \end{aligned} \quad (14)$$

- Fibre-Kinking failure;

$$\begin{aligned} \bar{E}_x &= k \cdot E_x \\ \bar{E}_y &= k \cdot E_y \\ \bar{E}_z &= k \cdot E_z \\ \bar{G}_{xy} &= k \cdot G_{yz} \\ \bar{G}_{xz} &= k \cdot G_{yz} \\ \bar{G}_{yz} &= k \cdot G_{yz} \end{aligned} \quad (15)$$

Where k is a degradation factor and the over-lined properties indicate the degraded values. The factor k is introduced to avoid convergence problems and to speed-up the progressive damage procedure. In the ideal case

$k=0$ but experience with this model shows that a practical value of $k=0.1$ is found to work very well. With this value of k , the material properties are degraded enough to consider them negligible, while at the same time the simulation is kept stable enough to reach the convergence at each step.

To avoid excessive element distortions and Jacobian singularity when failure in all plies occurs, the material properties for completely failed elements are increased in the normal contact direction in order to make the element incompressible under the contact pressure.

3 NUMERICAL PROCEDURE

The progressive damage approach, whose theory has been described in the last section, has been implemented in the in the commercial finite element code ANSYS.

A script file, written by using the ANSYS APDL language, integrates the ANSYS pre-processor, non-linear solver and general post-processor in order to carry out the iterative progressive damage procedure. The resulting numerical procedure is summarised hereinafter.

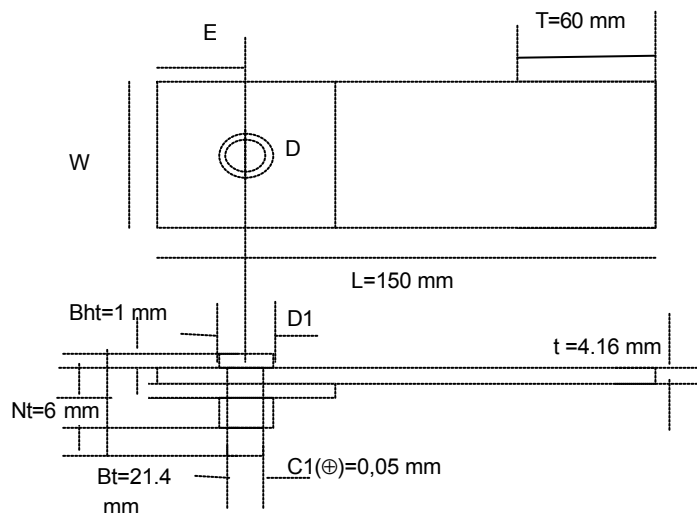
First, geometry, material layout, boundary conditions and initial loads are defined. A first linear step is carried out in order to evaluate the stresses for each layer of each finite element at the Gauss points. Then the resulting values are used to obtain layer average stresses. The layer average stresses are checked according to the above mentioned failure criteria. If failure does not occur the load is incremented while if failure occurs the material is properly degraded in all the damaged elements at ply level according to the ply discount rules. In both cases the convergence of the Newton-Raphson method, for the presence of geometrical and contact non-linearity, is checked to find the new equilibrium position related to the local change of material properties or to the increasing of load. In case of no convergence the structural collapse occurs, otherwise a new stress evaluation is performed.

The use of this numerical procedure makes it possible to monitor the progressive failure of composites in each ply and in each element from damage onset until global failure.

3 NUMERICAL APPLICATIONS ON SINGLE-LAP PROTRUDING JOINTS

3.1 Geometry, materials, FEM mesh, boundary conditions and applied loads

Among the different single-lap specimen tested in [22], three geometrical configurations with different diameters ($D=4.8$ mm and $D=6.4$ mm) and different interfaces (composite-composite and composite-aluminium) have been considered in the present paper for comparisons with numerical results and for numerical investigation on the structural behaviour of composite joints. The Geometrical description of the selected configurations is summarised in Figure 2.



Configuration n.	E/D	D1	W/D	D (mm)	Plates	Bolt
1	3	10.5	6	6.4	C/C	P
2	3	10.5	6	6.4	C/Al	P
3	3	7.8	6	4.8	C/Al	P

Figure 2. Single-lap specimen geometrical description.

The clearance (in agreement with the drawings in [22]) has been chosen $C1=50 \mu\text{m}$.
The properties of the materials of the joint's sub-components are presented in the following tables:

	Property	HTA 6376
Ply longitudinal modulus	E_1	145. GPa
Ply transverse modulus	E_2	10.3 GPa
Ply transverse modulus	E_3	11.1 GPa
In-plane shear modulus	G_{12}	5.3 GPa
Out-of-plane shear modulus	G_{13}	5.27 GPa
Out-of-plane shear modulus	G_{23}	3.95 GPa
Poisson's ratio	ν_{12}	0.3
Poisson's ratio	ν_{13}	0.5
Poisson's ratio	ν_{23}	0.5
Maximum ply tensile stress at 0°	σ_{1t}	2250 Mpa
Maximum ply tensile stress at 90°	σ_{2t}	64 Mpa
Maximum out-of-plane ply tensile stress	σ_{3t}	50 Mpa
Maximum ply compressive stress at 0°	σ_{1c}	1600 Mpa
Maximum ply compressive stress at 90°	σ_{2c}	290 Mpa
Maximum ply out-of-plane compressive stress	σ_{3c}	300 Mpa
Maximum ply in-plane shear stress	$\sigma_{12} = \sigma_{13}$	120 Mpa
Maximum ply out-of-plane shear stress	σ_{23}	50 Mpa

Table 1 : Material properties of composite plates.

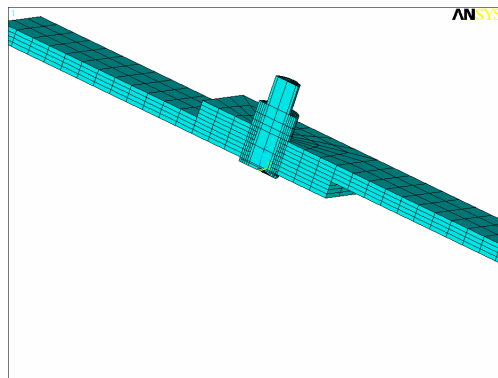
	Property	TITANIUM
Young modulus	E	110 GPa
Poisson's ratio	ν	0.29

Table 2 : Material properties of bolt and nut (titanium alloy).

	Property	ALUMINIUM
Young modulus	E	73.771 GPa
Poisson's ratio	ν	0.33 GPa

Table 3 : Material properties of aluminium plate (aluminium 2024 T351).

The specimens have been modelled using the ANSYS FEM code. The brick elements (BRICK 45) were used for bolt, nuts and aluminium plate while the layered brick elements (BRICK 46) were adopted to model the composite plates. A suitable mesh density was determined in order to minimise the computational cost without losing accuracy of results especially near the hole. The mesh density outside the overlapping zone was chosen to fit the extensometer's readings. In order to reduce the computational cost also the number of elements along the thickness was optimised. Four elements each with eight layers were placed along the thickness. The adopted mesh and the orientation of each ply are shown in figure 3.



Element	layer	Orientation
ELEMENT 4	8	9.0
	7	-4.5
	6	4.5
	5	0
	4	9.0
	3	-4.5
	2	4.5
	1	0
ELEMENT 3	8	9.0
	7	-4.5
	6	4.5
	5	0
	4	9.0
	3	-4.5
	2	4.5
	1	0
ELEMENT 2	8	0
	7	4.5
	6	-4.5
	5	9.0
	4	0
	3	4.5
	2	-4.5
	1	9.0
ELEMENT 1	8	0
	7	4.5
	6	-4.5
	5	9.0
	4	0
	3	4.5
	2	-4.5
	1	9.0

Figure 3. Single-lap specimen FEM mesh and composites stacking sequence

The surface-to-surface ANSYS contact elements have been used to take into account the contact-friction phenomena between the several interfaces (the frictional coefficient $\mu=0.2$ was chosen for all the interfaces). Using the penalty method the CPU cost needed in computations has been reduced but the choice of penalty parameter has become very difficult. To avoid convergence problems without losing anything in terms of accuracy it was necessary to perform a trade off analyses to find the right penalty parameters for the different interfaces (bolt-composite, composite-composite, nut-composite, aluminium-composite aluminium-bolt). In the next section the influence of penalty parameters on the quality of the numerical solution is discussed in detail. The boundary conditions applied to our model are schematically shown in the figure 4.

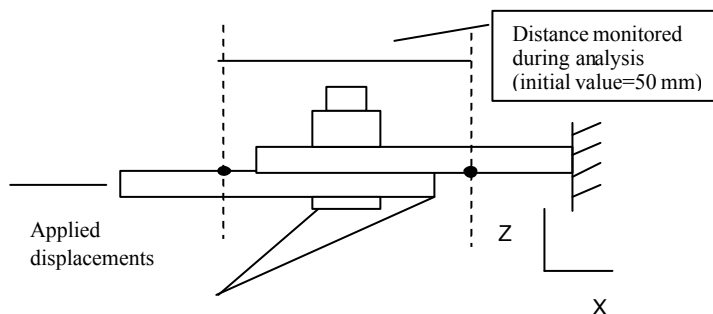


Figure 4. Boundary condition and applied load

As seen in the figure, one plate has been clamped while the other has been loaded by means of applied displacements.

Introducing elastic springs with a very low stiffness between a fixed point and the unconstrained sub-components of the joints, convergence problems due to the rigid-body motions (related to possible initial no-contact conditions) has been easily solved.

No bolt pre-load has been applied in the FEM model in order to analyse the worst-case scenario.

3.2 Numerical results

Numerical analyses have been performed on the selected three configurations in order to investigate the structural behaviour of protruding single-lap composite joints. The obtained numerical results have been compared with experimental data from [22] to check the effectiveness of the progressive damage procedure adopted in the numerical investigations.

A preliminary proof of the effectiveness of the optimised FEM discretisation has been given by the comparison of experimental strain gauges readings^[22] in some locations of the joint with the corresponding numerical results. The positioning of the strain gauges for configuration 1 and 2 is schematically presented in figure 5.

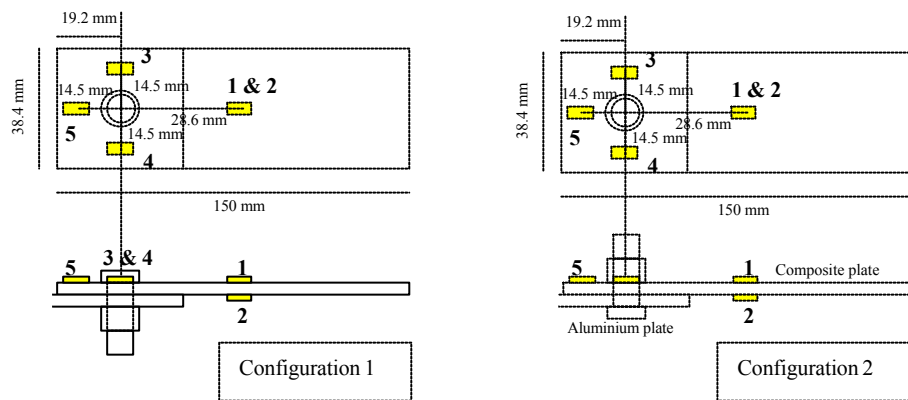


Figure 5. Positioning of strain gauges for configuration 1 and 2

Gauges 1 and 2 have been used to monitor the secondary bending outside the overlap region, gauges 3 and 4 have been used to monitor the secondary bending inside the overlap region and gauge 5 has been used to measure the strain due to bearing load from the bolt.

In figure 6 the comparison between experimental and numerical strains for configuration 1 is presented. For gauge 1, experimental readings show that the initial tensile strain due to tensile load is balanced by the compressive strain due to the secondary bending giving a total compressive strain as the tensile load increases.

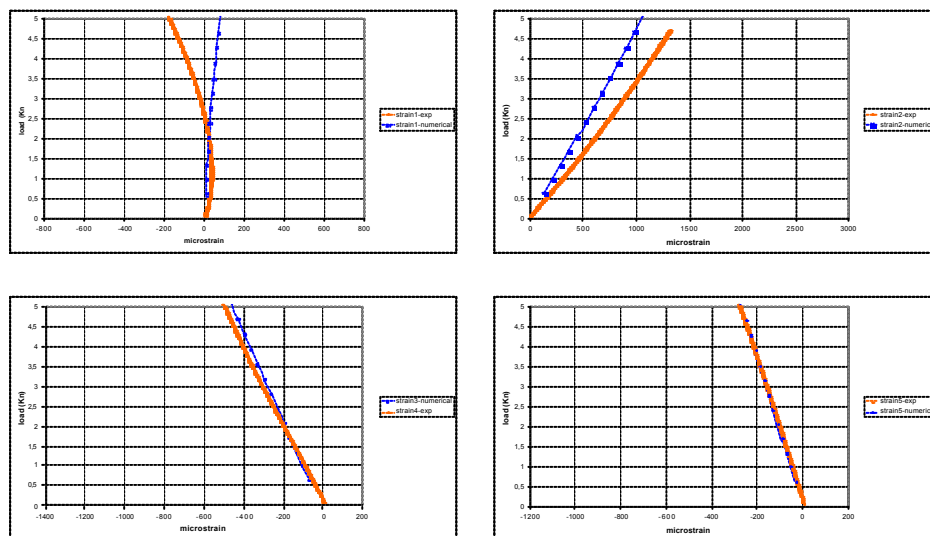


Figure 6. Comparison between experimental and numerical strains configuration 1

The numerical near zero value at this location indicates that the secondary bending phenomenon is slightly underestimated outside the overlap region. The same indication can be deduced by the comparison between the gauge 2 reading and the corresponding numerical value. The gauge 3 readings is in good agreement with the corresponding numerical result showing that the compressive strain due to the secondary bending in the overlap region is well predicted. Also the compressive strain due to bearing from the bolt is very well predicted by the proposed FEM approach as demonstrated by the excellent agreement between the gauge 5 readings and the corresponding numerical results.

In figure 7 the comparisons between experimental and numerical strains, for configuration 2, are presented. The same indications about the good prediction of the secondary bending inside the overlap region and about the slight underestimation outside the overlap region can be extrapolated.

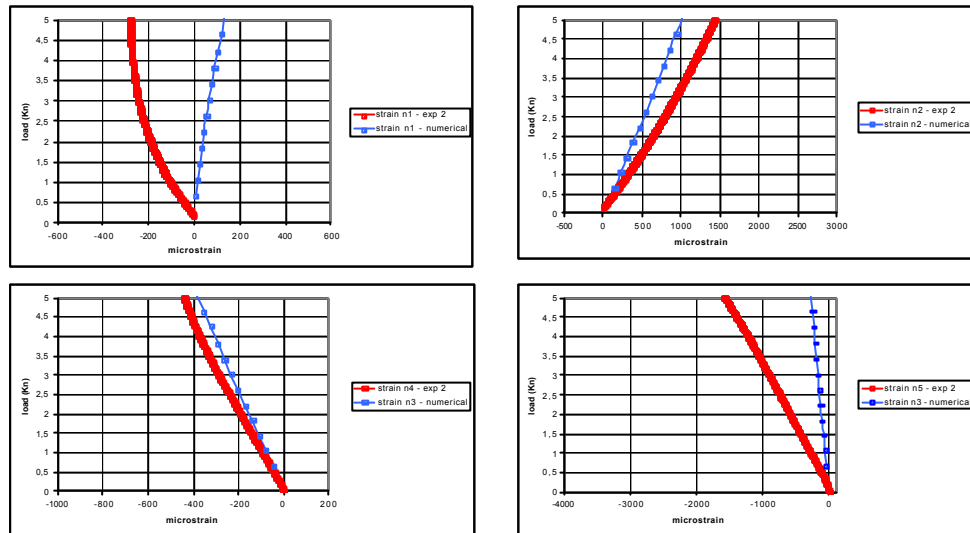


Figure 7. Comparison between experimental and numerical strains for configuration 2

For this configuration (composite-aluminium interface), differently from configuration 1, the comparisons between the gauge 5 readings and the numerical results show an underestimation of the compressive strain due to the bearing from the bolt.

Comparisons with experimental results in terms of load-displacement curves are also presented. In experiments^[22] an extensometer was attached to the mid-section of the joint. The gauge-length was 50 mm so both the legs of extensometer were outside the overlap region of the joint. From a numerical point of view, the distance between the two nodes of the longitudinal mid-section, shown in figure 4, has been monitored during analyses for comparison with experimental extensometer readings.

In figure 8 the comparison between experimental and numerical results for configuration 1 (composite-composite interface and $D=6.4$ mm) are presented in terms of applied load versus extensometer readings.

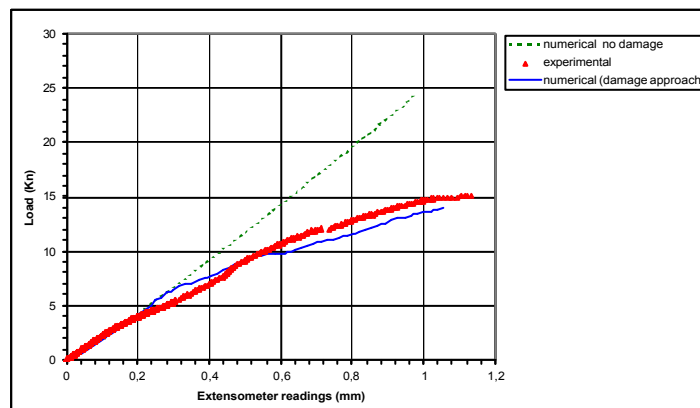


Figure 8. Configuration 1 - Applied tensile load versus deflection: experimental and numerical results.

The no-damage approach leads to a linear trend, which for large deflection, is very far from the experimental results. On the contrary, the proposed numerical progressive damage tool is able to follow the trend of experimental results.

The agreement between the numerical (with damage approach) and experimental results is excellent. The initial stiffness of the joint is well predicted. This is an additional proof of the effectiveness of the adopted FEM model and in particular of the chosen mesh density. On the contrary, the damage onset (that graphically can be characterised as the initiation of the non-linear trend) is slightly over-estimated. The uncertainty of the experimental determination of damage initiation and the singularity of the stresses at the hole-edge can be considered as the causes of this discrepancy.

The proposed numerical approach is able to simulate the continuous loss of joint stiffness, due to damage propagation and rotation of the bolt, until the final failure. However, some little differences between the experimental and the numerical curves and a slight under-estimation of the failure load can be appreciated in figure 8. Since the little uncertainties in experimental determination of material strengths' values were found to be not critical for this kind of joint, the reason for the above mentioned discrepancies can be found in the influence of contact penalty parameters and friction on the overall damage propagation.

The comparison between experimental and numerical results in terms of applied load versus extensometer readings for configuration 2 (composite-aluminium interface and $D=6.4$ mm) and configuration 3 (composite-aluminium interface and $D=4.8$ mm) is presented in figure 9.

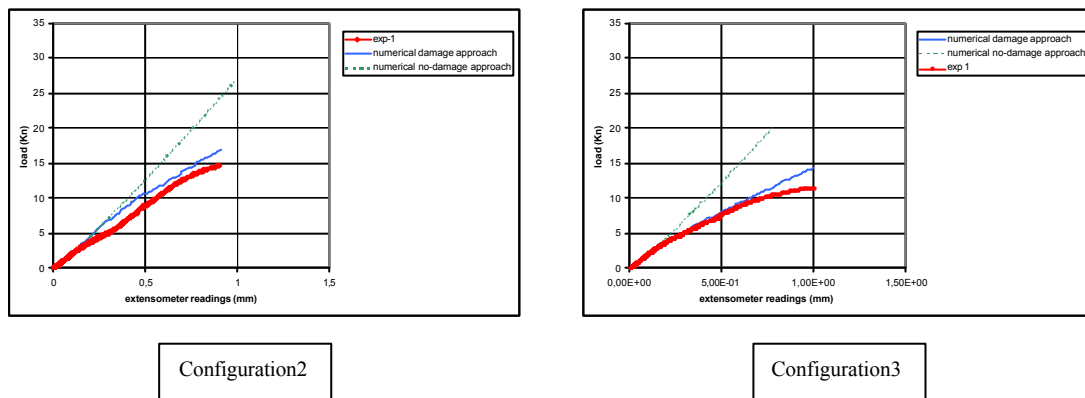


Figure 9. Configuration 2 and 3 - Applied tensile load versus deflection: experimental and numerical results.

As already pointed out for the previously analysed configuration, the proposed numerical progressive damage tool is able to follow the trend of experimental results. The agreement between the numerical (with damage approach) and experimental results is again very good. The initial stiffness of the joint is well predicted and for configuration 3 also the damage onset is excellently estimated. For these two configurations, the failure load is slightly over-estimated. The reason for this behaviour can be found in the lack of plastic deformations of the aluminium plate (occurred in experimental tests on configurations 2 and 3 due to the secondary bending) in our FEM model. However the overall agreement between experimental and numerical results is still very good.

To investigate the influence of contact stiffness (penalty parameter in the penalty formulation) on the of the joint's numerical response, a comparison between load-displacement curves for configuration 1, calculated using different penalty parameters, is presented in figure 10.

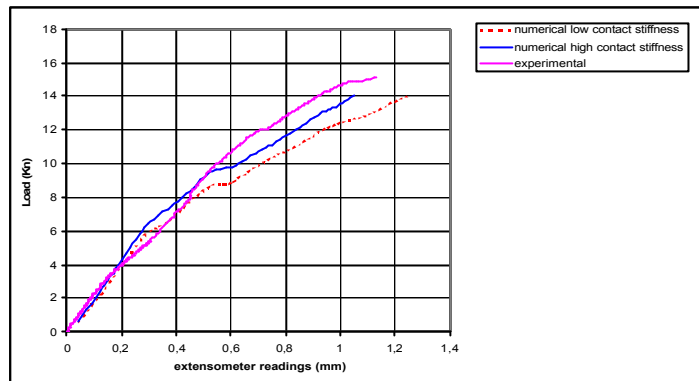


Figure 10. Configuration 6 – Influence of contact stiffness on the joint’s response.

The initial slope of the curve, that represents the initial stiffness of the joint, is under-estimated using low values of the penalty parameter, consequently the onset and the progression of damage obtained by means of low penalty parameters is far from the experimental ones. So the use of high values of penalty parameter is recommended in order to fit in a better way the experimental results. However there is a limit value of penalty parameter beyond which the convergence is not assured anymore. This limit value allows a penetration that can substantially influence the contact pressure distribution at bolt-hole interface leading to slight deviations from experimental results.

The importance of contact phenomena for the problem under investigation is pointed out also in figure 11 where the deformed shapes of configuration 1 are introduced. Since the deformed shapes of configuration 2 and 3 are very similar, for sake of compactness they will be not presented. From this figure also the secondary bending can be appreciated.

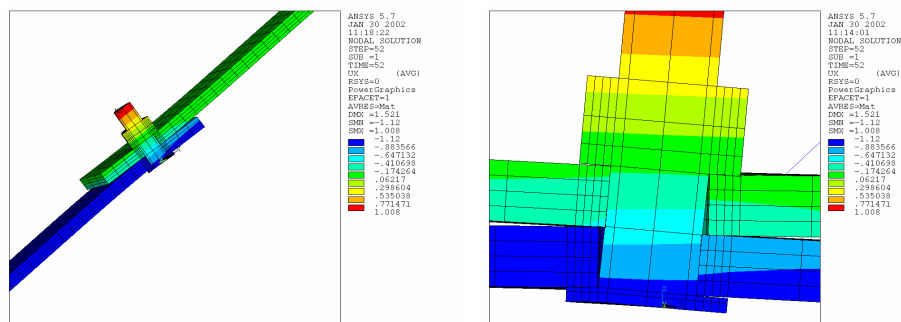


Figure 11. Deformed shapes – (isometric and cut views) configuration 1 –Applied $U_x = 1.26$ mm

The normal contact pressure, The friction contact stress and contact penetration distributions along the surface of the hole at the last computed load step (Applied $U_x = 1.26$ mm) for the configuration 1 are well represented in figure 12 (the distributions for configuration 2 and 3 are again very similar).

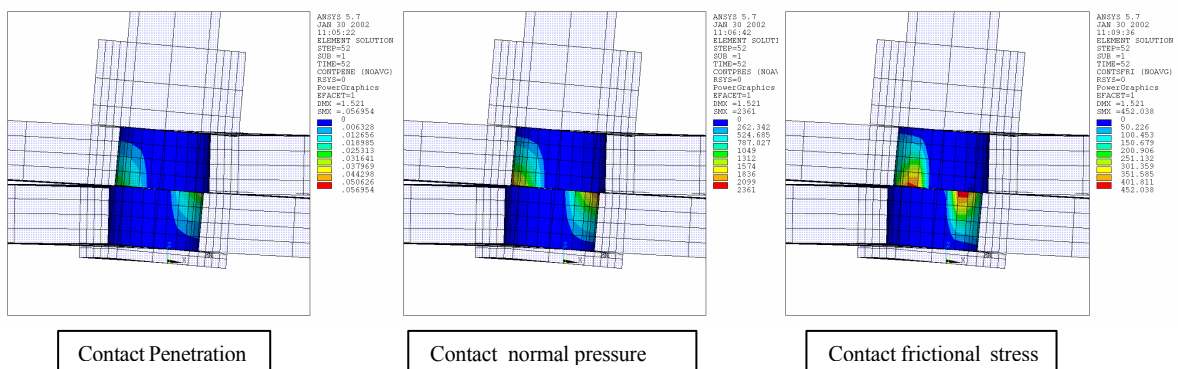


Figure 12. Contact penetration, contact pressure and contact frictional stress for configuration 1- $U_x = 1.26$ mm

As proof of the right choice of the penalty parameters, the computed contact penetration is very small if

compared with the deflection of the joint (max penetration for $U_x = 1.260$ mm is 0.056 mm). The most critical regions for contact analysis are located between bolt and hole at the interface of the composite plates near the hole edge and between the bolt head/nut and the composite plates. In these regions the choice of the penalty parameter has been found determinant for the convergence speed. The frictional contact stress distribution has been found to be very similar to the one presented in [23].

To show the details about the damage evolution inside the composite joints, some pictures are introduced, showing the percentages of broken laminae in the elements at different load steps. In Figure 13 the failed elements for the configuration 1, at two load steps ($U_x = 0.64$ mm - tensile load = 9,06 Kn and $U_x = 1.26$ mm - tensile load = 14,03 Kn) are shown.

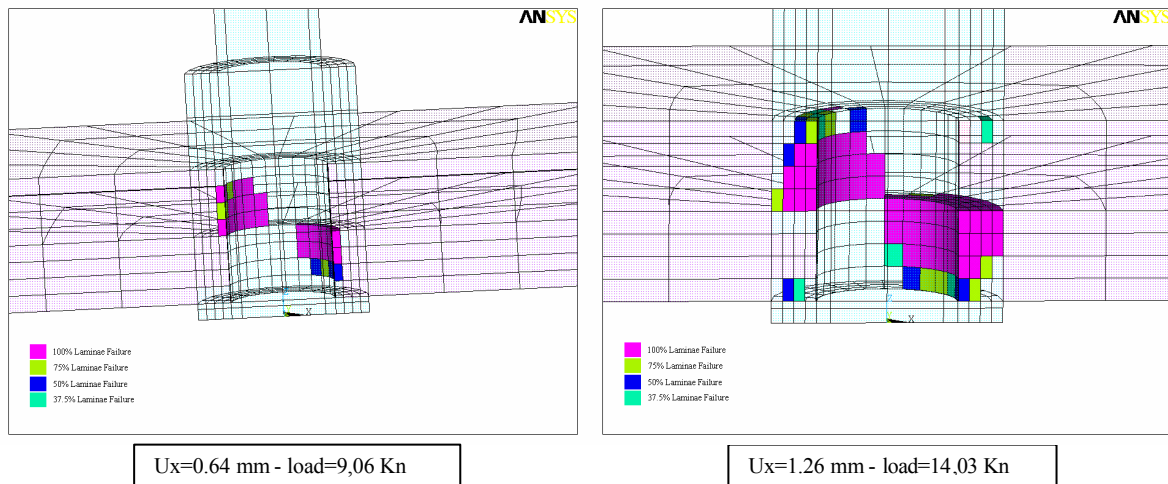


Figure 13. Configuration 1- Percentage of broken plies in elements at two load steps.

The failure onset takes place at the interface between composite plates near the hole edge where the contact pressure reaches its maximum value (see figure 12). The effect of the compressive stresses acting on the hole surface in the contact region between hole and bolt is the initial matrix cracking at hole edge interface.

As the load increases, the fibres compressive breakage and the fibres kinking become relevant in the vicinity of the hole. The propagation of damaged area in the radius direction is more relevant near the composite plate interface at the hole-edge. The onset of damage between the bolt head /nut and the composite plates due to the kinking breakage mechanism is also appreciable.

The deformation at the composite hole edge, caused by damage accumulation, leads to an increase of the contact area between bolt and hole. So the damage (matrix cracking, fibres compressive breakage and fibres kinking) extends towards the composite external surfaces.

The damage evolution of configuration 2 is shown in figure 14 where the failed elements at two load steps ($U_x = 0.56$ mm - tensile load = 9,28 Kn and $U_x = 1.12$ mm - tensile load = 16,40 Kn) are shown.

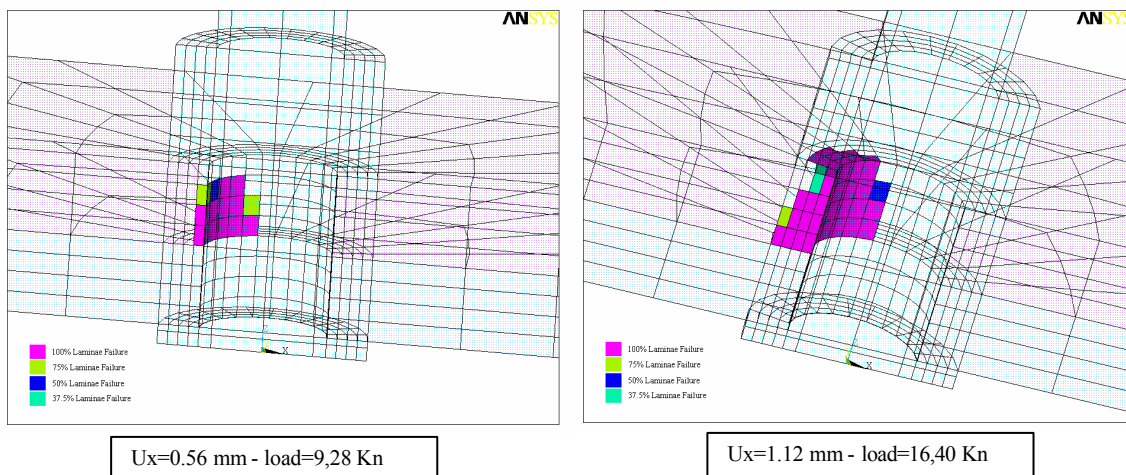


Figure 14. Configuration 2- Percentage of broken plies in elements at two load steps.

The damage propagation, at the first load step doesn't show appreciable differences from the one observed for configuration 1. However, at the last computed load step, unlike the configuration 1, the propagation of damage in the radial direction is quite constant along the plate thickness. This different distribution can be related to the different evolutions of contact areas between bolt and hole, during the propagation of damage, for the two analysed interfaces (the presence of aluminium plate seems to forces the damage to be quasi-uniformly distributed along the composite plate thickness). The damage evolution of configuration 3 is very similar to the one of configuration 2 so it has not been presented.

In figure 15 some experimental ultrasonic NDE results on configuration 1 are presented in order to compare the damage propagation predicted by means of our numerical tool with the experimentally measured one.

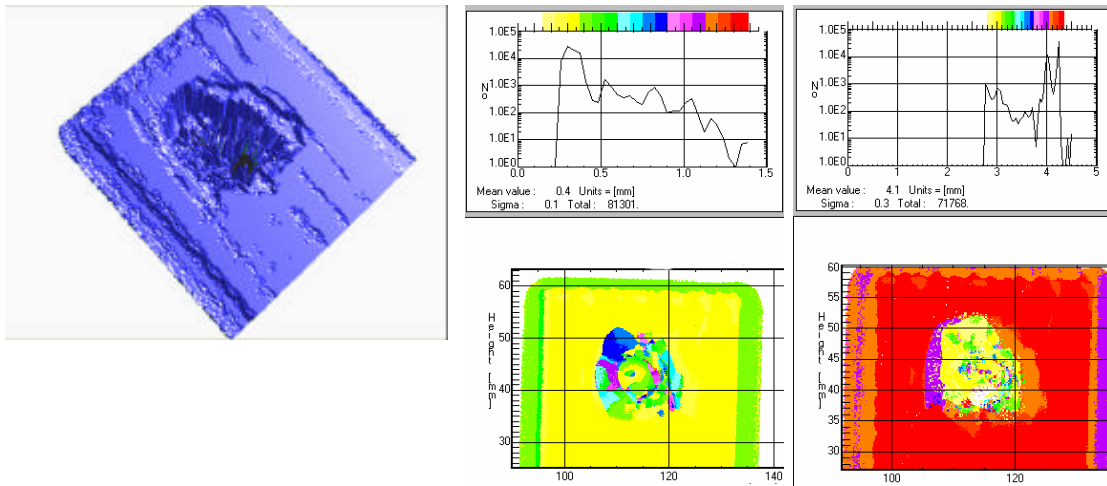


Figure 15. Configuration 1 NDE inspections - Applied $U_x = 1.26$ mm

In this figure a three-dimensional representation of the damage location along thickness, starting from the interface between composite plates, is shown. In the same figure Also the experimental ultrasonic NDE results (in terms of time of flight) for the failed configuration 1 specimen at two different thickness intervals from external surfaces to the interface between composite plates are presented.

The trend shown by experimental data is in agreement with numerical results showing a concentration of the damage at the hole-edge near the composite plates' interface. Along the thickness is clearly visible a reduction of the damaged as we move towards the external surface of composite plates. It should be pointed out that our numerical model is not able to predict the delaminations' onset and propagation appearing in the NDE analysis especially near the external surface.

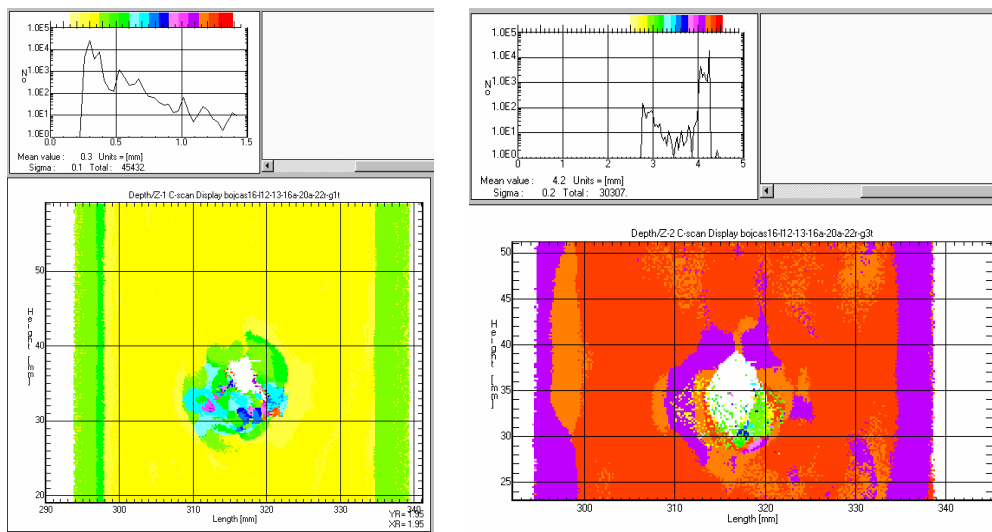


Figure 16. Configuration 2 NDE inspections - Applied $U_x = 1.12$ mm

In figure 16 the distribution of damage at two different thickness intervals for configuration 2 is presented. The trend of figure 15 is again in agreement with numerical results showing a concentration of the damage near hole-edge at composite plate interface and a rather constant distribution of damage along the thickness.

4 CONCLUSIONS

A detailed numerical investigation on the structural behaviour of single-lap protruding composite joint has been presented. A progressive damage approach has been adopted in order to investigate the damage onset and evolution in the analysed composite joints. The proposed methodology has been verified by using the experimental results of three different geometrical configurations of single lap specimens tested in tension.

Preliminary comparisons in terms of strain curves between experimental and numerical results have confirmed the effectiveness of the adopted FEM discretisation.

Further comparisons among the numerical no-damage approach, the progressive damage approaches and the experimental results in terms of tensile load vs. extensometer readings have shown that, for all the configurations, the non-linear no-damage approach is inconsistent and ineffective to predict the real structural behaviour of the joints. On the contrary the progressive damage approach demonstrated a remarkable capability to follow the non-linear experimental trends. The slight deviations from the experimental trends due to the singularity of the stresses at the hole-edge and due to the lack of plasticity of aluminium plates in the proposed FEM model, don't affect in a relevant way the overall numerical prediction.

For the analysed configurations the contact phenomena have been investigated. The contact penetrations, the contact pressures and the frictional contact stresses have been monitored in detail. Comparisons between different analyses on configuration 1 with different penalty parameters have been performed to show the influence of contact penalty parameters on the numerical predictions.

The damage onset and propagation have been monitored during analysis and has been found almost the same for all the analysed configurations. Some differences in the damage distribution along the plate thickness, at the final stage of the loading process, between the composite-composite and the aluminium-composite joints have been observed and critically discussed. The trends of numerically evaluated damage progression have been fully confirmed by comparisons with ultrasonic C-scan measurements.

In conclusion the progressive damage approach proposed in this paper has been demonstrated to be affordable and effective for the detailed models of composite joints. Future work could be addressed to the inclusion of delamination on-set, delamination propagation and plasticity of the aluminium plates.

ACKNOWLEDGEMENTS

Part of the work presented in this paper was performed in the frame of BOJCAS.

BOJCAS - Bolted Joints in Composite Aircraft Structures is a RTD project partially funded by the European Union under the European Commission GROWTH programme, Key Action: New Perspectives in Aeronautics, Contract N° G4RD-CT-1999-00036.

REFERENCES

- [1] Waszczak, J. P. and Cruse, T. A. (1971), "Failure mode and Strength Predictions of Anisotropic Bolt Bearing Specimens", *J. of Composite Materials*, Vol. 5, pp. 421-425.
- [2] Agarwal, B. L. (1980), "Static Strength Prediction of Bolted Joint in Composite Material", *AIAA Journal*, Vol. 18, pp. 1345-1375.
- [3] Soni, S. R. (1981), "Failure Analysis of Composite Laminate with a Fastener Hole", *Joining of Composite Materials*, ASTM STP 749, K.T. Kedward, Ed. Am. Soc. for Testing and Materials, pp. 145-164.
- [4] York, J. L., Wilson, D. W. and Pipes, R. B. (1982), "Analysis of Tension Failure Mode in Composite Bolted Joints", *Journal of Reinforced Plastic and Composites*, Vol. 1, pp. 141-153.
- [5] Wilson, D. W. and Pipes, R. B. (1981), "Analysis of Shear-out Failure Mode in Composite Bolted Joints", *Proceedings of the 1st International Conference on Composite Structures*, Paisley College of Technology, Scotland, pp. 34-49.
- [6] Collings, T. A. (1982), "On the Bearing Strengths of CFRP Laminates", *Composites*, Vol. 13, pp. 242-252.
- [7] Chang, F. K. and Scott, R. A. (1984), "Failure of Composite Laminates Containing Pin Loaded Holes – Method of Solution", *J. of Composite Materials*, Vol. 18, pp. 255-278.
- [8] Yamada, S. E. and Sun, C. T. (1978), "Analysis of Laminate strength and Its Distribution", *J. of Composite Materials*, Vol. 12, pp. 275-284.
- [9] Lessard, L.B. and Shokrieh, M.M. (1995), "Two-dimensional Modelling of Composite Pinned-Joint Failure",

- Journal of Composite Materials, Vol. 29, pp. 671-697.
- [10] Kim, S.J. and Hwang, J.S. (1998), "Progressive Failure Analysis of Pin-Loaded Laminated Composites Using Penalty Finite Element Method", *AIAA Journal*, Vol. 36, pp. 75-80.
 - [11] Hashin, Z. (1980), "Failure Criteria for Unidirectional Fibre Composites", *Journal of Applied Mechanics*, Vol. 47, pp. 329-334.
 - [12] Zhong, Z.H. (1993), *Finite Element Procedures for the Contact Impact Problems*, Oxford Science Publications.
 - [13] Murray, Y. and Schwer, L. (1990) "Implementation and Verification of Fiber-Composite Damage Models", *Failure Criteria and Analysis in Dynamic Response*, ASME AMD, Vol. 107, pp. 21-30.
 - [14] Colvin, G. E. and Adams, D. S. (1986), "A Finite Element Overlay Technique for Modelling Pinned Composite Joints", *AIAA* 86-1420.
 - [15] Chen, W-H., Lee, S.S. and Yeh, J-T. (1995), "Three-dimensional Contact Stress Analysis of a Composite Laminate with Bolted Joint", *Composite Structures*, Vol. 30 pp. 287-297.
 - [16] Camanho, P.P. and Matthews F.L. (1999), "Delamination Onset Prediction in Mechanically Fastened Joints in Composite Laminates", *Journal of Composite Materials*, Vol. 33 pp. 906-927.
 - [17] Ireman, T. (1998), "Three-dimensional Stress Analysis of a Bolted Single-lap Composite Joint", *Composite Structures*, Vol.43 pp. 195-216.
 - [18] Kermanidis, Th., Labeas, G., Tserpes, K.I. and Pantelakis, Sp. (2000), "Finite Element Modelling of Damage Accumulation in Bolted Composite Joints Under Incremental Tensile Loading", *ECCOMAS 2000*.
 - [19] Perugini, P., D'Anna, G., Riccio, A., Scaramuzzino, F. and Tessitore, N. (1999), "Progressive Failure Analysis of Composite Joints", *ASME conference, Virginia US*.
 - [20] Perugini, P., Riccio, A. and Scaramuzzino, F. (2001), "Three-dimensional Progressive Damage Analysis of Composite Joints", *Proceeding of the Eighth International Conference on Civil and Structural Engineering Computing in Eisenstadt (Vienna)*, Civil-Comp Press, Stirling, Scotland, 2001.
 - [21] Riccio, A., Perugini, P., Scaramuzzino, F., McCarthy, M. and Stanley, W. (2001), "Three-dimensional Modelling of Progressive Damage in Composite Joints", submitted for publication on *Computers & Structures*.
 - [22] Riccio, A., Lizza, A., Ferrigno, A. and Marciano, L. (2002), "Single-lap and double-lap Composite Joints Tensile Test Results," Deliverable D5-6 BOJCAS (Brite-Euram /Bolted Joints in Composite Aircraft Structures).
 - [23] Kim, S. J. and Hwang, J.S. (1998), " Progressive Failure Analysis of Pin-Loaded Laminated Composites Using Penalty Finite Element Method," *AIAA Journal*, Vol. 36 pp.75-80.